Distant Galaxies Science Case for MCAO

Simon Morris (DAO/HIA/NRC),
Inger Jørgensen (Gemini),
Ray Sharples (U. of Durham),
Francois Rigaut (Gemini), and
Mark Chun (Gemini).

1 INTRODUCTION

A variety of science cases were considered in the document justifying the construction of Altair for Gemini (Morris et al. 1996). These science cases were revisited in the Altair Operational Concepts Definition Document (Morris, Herriot and Davidge 1997), where 5 cases were considered in more detail. In parallel with this effort, a meeting was held at Abingdon in January 1997 where the science drivers for the Gemini On-Going Instrumentation Plan (OGIP) were formulated (Gillett et al. 1997). In none of these Gemini documents was the possibility of wide FOV AO considered. However, it is certainly clear that many of the science cases considered would benefit substantially from MCAO. From the list in Table 1 of the Altair OCDD, clear cases of this in the distant galaxies area are:

- Starburst galaxies - many of the nearer starburst galaxies subtend more than an arcminute, while individual giant HII regions in these objects are < 1 arcsecond in diameter. Spatially resolved spectroscopy across the extent of these galaxies will allow us to understand the triggering and propagation of the star formation. (It should be noted that the above arguments also apply for galaxies not currently undergoing starbursts - where one might wish to still study the star formation process).
- Gravitational arcs - while individual giant arcs are generally only a few arcseconds along their long dimension, and entire set of images for a given background galaxy may well be spread over an arcminute or more. Spatially resolved spectroscopy of all of these images will allow detailed reconstruction of the high redshift lensed galaxy, with information on scales that will be unobservable in any other way.
- High redshift galaxies and clusters - we will explore this case in much more detail below, but the cores of moderate redshift clusters of galaxies subtend a few arcminutes, while the comoving volume from which objects such as the local group were likely assembled also subtends this sort of scale at high redshifts. Smaller fields of view, while valuable, will often require mosaicing in order to map out the scientifically required region.

In the Abingdon report, science areas identified as benefiting strongly from wide FOV are called out in their Table 2, and in every case these projects are also listed as benefiting from AO. The MCAO offers the chance to get both of these benefits at once. The distant galaxies cases so identified therein are:

- Evolution of galaxies
- Galaxies as probes of high z structure

A third fruitful source for science cases for MCAO comes from what will no doubt eventually (in 2009) be its main competitor. The Next Generation Space Telescope (NGST) has had a huge amount of effort put into its science requirements. The culmination of this effort is the Design Reference Mission (DRM), in which three years of 8m telescope time in space is allocated amongst projects that a large group thought would be forefront astrophysics in 2009. Scanning that list of observations (available on the web), there are extremely few which are targeting single, small objects. The vast majority request imaging over FOV greater than a few arcminutes, or multi-object or IFU spectroscopy over similar sizes regions. With MCAO on Gemini, despite the higher background from its location on the ground, and also a significantly smaller effective FOV, a reasonable fraction of these DRM programs can be attempted well in advance of the launch of NGST. Particularly exciting examples of this in the distant galaxies area include, high-z supernovae searches to accurately determine Λ, observations of the host galaxies of Gamma-ray bursters (where one needs the MCAO FOV to be sure one covers the gamma ray error circle), and both imaging and low resolution spectroscopy in the NIR to study galaxy evolution and hierarchical clustering.

2 BASIS FOR COMPARISON

For any MCAO science case (ignoring for now cases that require specific access to targets only visible from either the N or S), one has to consider the following modes for doing the science with Gemini:

1. Gemini N or S with TT correction only
2. Gemini N with Altair and NGS
3. Gemini South with Hokupa'a 85 and NGS
4. Gemini N with Altair and LGS
5. Gemini S with Hokupa'a 85 and LGS
6. Gemini S with MCAO

As can be seen from the long list of choices, the decision may well not be a simple one. Also, reliable performance estimates for all of these systems are not yet available. Indeed, given the careful site monitoring campaign and the detailed analysis presented in this CoDR, the MCAO performance may be one of the better known.

That said, some qualitative statements to help the trade can be made.

a) TT alone will give almost complete sky coverage with a FOV of up to 7'. The (relatively broad) PSF will vary slowly with distance from the TT guide star.

b) There is a throughput and emissivity penalty for any Gemini AO correction beyond simple TT.

c) Gemini N seems to have slightly better natural seeing than Gemini S, with **possibly** a single dominant turbulence layer for a significant fraction of the time. Should these situations happen to occur, the Altair anisoplanatism will be greatly reduced (i.e. the PSF will vary slowly across the 2 arcmin diameter FOV.

d) On-axis NGS performance will be slightly better than on-axis LGS performance as measured by Strehl.

e) NGS sky coverage will always be a lot lower than LGS. Interestingly, the MCAO sky coverage is comparable to that for single LGS AO, due to the trade between the smaller FOV of single LGS AO versus the need for 3 NGS for MCAO.

f) LGS will have to be turned off if clouds could potentially be hiding nearby aircraft, and may not work if cirrus along the LOS causes confusion in the returning laser signal.

We also need to keep in mind a realistic instrument complement for MCAO. Ideally this would include a well-sampled NIR imager covering the maximum possible FOV. For Nyquist sampling at 1 micron this implies 4.7kx4.7k pixels to cover 1x1 arcmin. Such sampling may well be overkill for the distant galaxies science, but if it is significantly degraded then it has to go into the Strehl budget as another cause of loss of image quality. One would also like deployable multiple IFU spectrographs also patrolling a 2x2 arcminute FOV. For imaging, conservative calculations for Hokupa'a on Gemini N indicate we will obtain S/N=5 per pixel for galaxies with integrated Kprime magnitudes of around 20 (K(AB)=22). In a ½ magnitude wide bin around this flux level there are between 5-10 galaxies per square arcminute in the field. For spectroscopy, the flux limit for pure continuum sources will be higher, but for emission line objects, will probably be roughly comparable. Some detailed calculations of the possibilities for observations of z=1 galaxies in Hα are given in the Gemini NIFS CoDR documentation, showing that in 1 hour it will be possible to measure the rotation curve of a z=1 galaxy in Hα.

The surface density of galaxies which are well matched to any given science project is probably too low to take full advantage of the MCAO multiplex gain, probably making it necessary to take yet a further step in the direction of queue-type observing already being blazed by Gemini. One will want to consider merging proposals not only within a night, but even within a single multiple IFU exposure with MCAO. One can imagine simultaneously obtaining Hα rotation curves for a few z=1 galaxies in the J band, looking at the kinematics in [OII] in the K-band for a z=4.5 galaxy and estimating the SNR rate using diagnostic NIR lines in a z=0.5 galaxy in the H-band, where each target had its own IFU. The logistics of such merging may prove horrendous, but the long spectroscopic exposure times (probably up to a night), and high costs of MCAO, make investigating such ideas necessary.

For the science cases below we will try to keep the above trades in mind at all times, although producing quantitative comparisons (such a number of nights needed to produce

a scientific result for each hardware option above) has not been possible with the time and personnel available. However, in section 4 we discuss based on similations the numerical gains for faint galaxy photometry and morphology measurements for MCAO compared to classical AO.

3 SCIENCE GOALS

Below we give a few illustrative examples of how studies of galaxy formation and evolution benefit from MCAO.

3.1 Location of Merging Fragments

Figure 3.1 shows the results from an HST study by Pascarelle et al (1996). They used a 0.15 micron wide filter to identify objects with Lyman-α emission at z=2.39 associated with a weak radio galaxy. The figure shows 18 candidate 'fragments' spread across a 2.5 arcminute diameter field (corresponding to 0.7 Mpc for h=0.8, q_0=0.5). At least 8 of these fragments have been confirmed spectroscopically, and have been shown to have a relatively small dispersion in velocities (~300 km/s). It has therefore been claimed that these fragments will have merged to form an early type galaxy by the present day.

It is clear from Figure 3.1 that identifying all such fragments will be extremely arduous without MCAO. After identifying the candidate fragments using photometric redshifts, one would then like to follow up a subset of these fragments at higher spectral resolution in order to measure their velocities and velocity dispersions (masses).

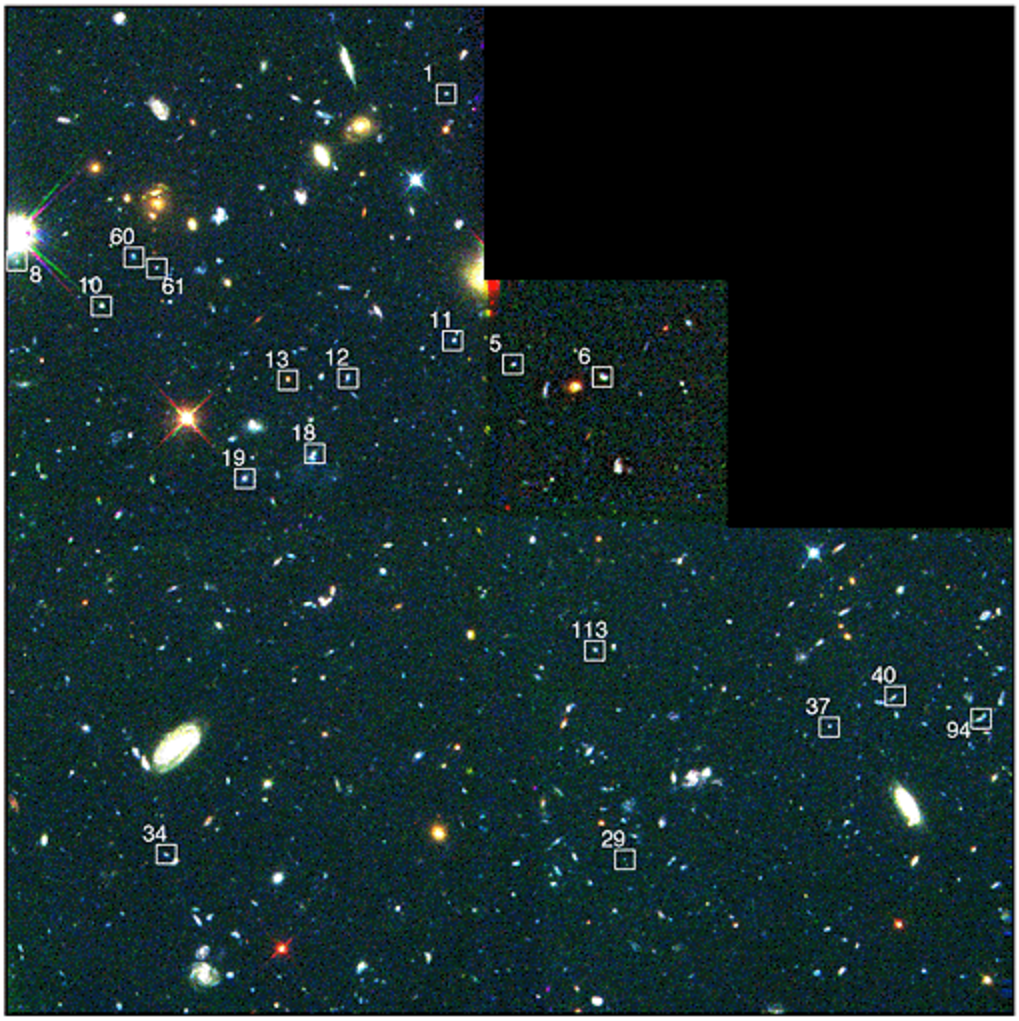

The boxes in this color image identify 18 sub-galactic sized objects in a Hubble Space Telescope survey of faint galaxies. All the boxed objects are at the same distance from Earth (11 billion light-years), and are scattered across an area of sky 2 million light-years across. They are close enough to each other they may eventually merge to form normal galaxies.

Credit: Rogier Windhorst (Arizona State University) and NASA

Figure 3.1: Merging galaxy fragments. Pascarelle et al 1996.

3.2 Formation of the Hubble Sequence

It has long been known that the morphologies and star formation histories of galaxies are strongly correlated with their environment. Red elliptical galaxies dominate rich clusters of galaxies, while the field contains predominantly blue spirals. More recent work has

shown that this correlation is seen even within the 'field' population (Hashimoto et al. 1998), where the star formation and morphologies of galaxies within small groups or generally slightly over-dense regions are also significantly different from those of galaxies in low density regions. The Hashimoto et al. study used the LCRS sample of 15,000 galaxies spread over a large angle on the sky, but limited to redshifts less than 0.2. Huge samples of galaxies will be needed to measure the local galaxy density. Again the wide field of MCAO (or more) will be needed for efficient observation.

Three rather general points can be made about the benefits of large samples of galaxies with relatively complete spectroscopic information:

1. Such samples make possible the finding of rare and unusual galaxies. Some possible examples of such objects would be very high redshift galaxies, Ultra-Luminous Infra-Red Galaxies, or low-luminosity, low star-formation rate dwarfs.
2. Another general area needing large samples is anything where one would like to break the galaxy sample into several bins. Immediately obvious cases of this are studies of the star formation rate as a function of redshift, or the evolution in galaxy metallicity with redshift. For both of these one would like to break the galaxy sample into several bins in luminosity, morphological class, and possibly also spectral class. This division (on top of binning in redshift) will rapidly reduce a sample of a few hundred galaxies to statistical meaninglessness.
3. Selection effects often plague studies of galaxy evolution. Substantial samples are needed to quantify and correct for any such effects.

It is also true that high spatial resolution, wide FOV, data will undoubtedly prove to be a rich source for serendipitous discoveries.

3.3 Star formation in galaxies at z~1-3

Over the last several years great strides have been made in finding galaxies at very high redshifts and estimating the star formation history of the universe (cf. Steidel et al. 1996, Madau et al. 1996). The emerging picture of the history of star formation in galaxies in the universe suggests that the star formation rate was higher in the past than measured locally; the star formation rate has decreased for redshifts less than $z \sim 2$ by a factor of about 10. Beyond a redshift of z~2, dust, AGN contributions, and use of different diagnostics make the picture more difficult to interpret. However, a deviation from an increasing star formation rate with redshift occurs around z~1 to z~3. The gap in observations at this redshift is due to the shift of the key optical diagnostic lines into the near infrared. For example, the most direct measure of the current star formation rate. Using the hydrogen recombination line $H\alpha$, becomes difficult with optical data at around z~0.5-1. Use of optical diagnostic lines such as $H\alpha$, $H\beta$, and [OIII]5007 are important since they are less sensitive to dust, the major unknown in estimations of the star formation rate using the UV continuum. Note that the use of [OIII] used in conjunction

with the hydrogen recombination lines also gives a handle on the metallicity in these systems.

With a multi-conjugate adaptive optics system with good performance throughout the near-infrared and a multi-object spectrograph, Gemini will be able to explore this redshift range with a great multiplexing advantage. An ability to resolve emission originating from the core and from discrete HII regions in the outer portions of the galaxies is obtained for resolutions of ~0.1". (The minimum angle subtended by a 1 kpc region due to the curvature of space is 0.2" (for h=0.8 and q_0=0.5).) Assuming a conversion factor of 10^{41}erg/s per M_{sol}/yr in star formation (Kennicut 1983), we find that on Gemini, Hα can be observed (5σ, 3600sec) out to redshifts z~2.5 for galaxies with a total star formation rate greater than 1 M_{sol}/year. As the galaxy will be resolved, this corresponds to detection of the brightest HII regions in galaxies out to z~2.5 (assuming no evolution). In order to study field and cluster galaxies in a systematic way, we need the multiplexing capability of multi-object spectroscopy. If we assume that the density of galaxies is the same as locally, then there should be ~2-10 L* galaxies per square arcmin within the redshift range 1<z<3 (Thompson et al. 1994).

3.4 Search for high redshift galaxies

The high density of faint sources seen in the Hubble Deep Fields suggests that we may have detected a population of pre-galactic halos from which present-day galaxies were assembled. Until the advent of 50-metre telescopes and NGST, however, determining the redshifts, luminosity distributions and star-formation rates of these ultra-faint (R>25 mag, H>21) sources using direct spectroscopy will be extremely difficult, and limited to galaxies selected in the UV, whose spectra have strong absorption or emission features.

An alternative method to construct large redshift surveys of galaxies at faint magnitudes is to use the weak-shear gravitational lensing signal produced by massive clusters of galaxies (Fig. 3.2). When viewed through the core of an intermediate-redshift cluster, the images of background field galaxies appear as distorted and magnified arclets, whose strength depends on both the mass distribution of the lensing cluster *and* the redshift of the background source. Kneib et al. (1996) have shown that this degeneracy can be broken by using detailed cluster mass models derived from the positions, shapes and redshifts of a few strongly-lensed giant arcs and multiply-imaged sources. This inversion technique is purely geometrical, and does not suffer from the selection biases associated with the identification of spectral features. By measuring the arclets in the infrared (H-band), one can also avoid any biases due to optical (rest-frame UV) selection. The redshift precision (5-10%) depends on the strength of the image distortion, and hence would also benefit significantly from the stable diffraction-limited PSF of MCAO. At H=23 (10σ 1hr) we expect a surface density of ~20 arclets per arcmin^2, of which ~1/4 are expected to be at z>1, allowing the first determination of the form of the (rest-frame) optical luminosity function at these redshifts down to faint luminosities (L^*+1.5 at z=2).

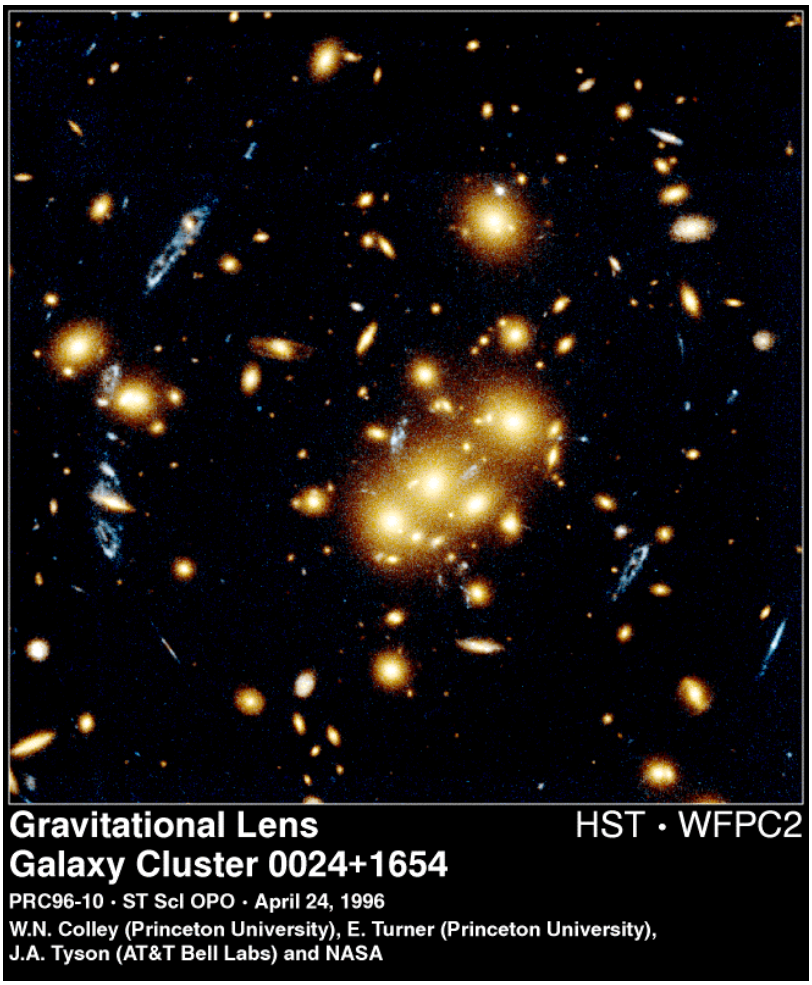

Figure 3.2: Multiple images of a background ring galaxy can be seen. This cluster does not have a suitable star for NGS AO, and the images above are spread over a large enough region to require MCAO.

Many of the lensed objects have very small angular sizes; often less than one arcsecond. Thus, in order to study the lensed objects in any detail, superior spatial resolution is needed. There are examples of cases where reconstruction of spatial appearance in the source plane has been attempted based on HST/WFPC2 data. The lensed objects found with optical data often have redshifts less than 1-1.5. However a few very high redshift objects have been found (Ebbels et al. 1996).

The typical spectral energy distribution of galaxies (especially those that are dominated by old stellar populations) makes it very hard to detect galaxies with redshifts from about 1.3 to 2.2 using optical data. [At redshift 1.3 the 4000A break is redshifted too far into the red to be observable with optical observations. At redshifts larger than 2.2 the Ly-alpha line becomes observable in the optical.] As a result very little is known about stellar populations in galaxies with redshifts in this interval. Studying these galaxies should be

possible using spectroscopy in the near-IR - and searching for them as lensed objects behind rich intermediate redshift clusters should make the task easier.

The candidate high redshift galaxies may be identified in three ways: (1) redshift 2.3-4.0 based on the 4000 A break and dropouts in J and/or H, (2) redshifts from 1 to 4 based on the near-IR colors. (3) We may also have the possibility of detecting galaxies at even higher redshifts based on the dropout method. There are breaks in the UV that at very high redshifts will be observable in the near-IR.

A large field, e.g. >1'x1', is very important for the success of such a search. For example, with 2'x2' we could carry out the search for high redshift galaxies behind the core of a cluster at redshift around 0.5 with one field observed. Since these high redshift galaxies may be very difficult to find it is essential to have a large field of view.

Once candidate high redshift galaxies are found, follow-up spectroscopy may be possible for the brightest candidates. The spectroscopy will also benefit greatly from the AO. In fact, such observations are most likely impossible without AO due to the small angular size of the lensed galaxies combined with the bright background in the near-IR.

A complimentary field of study for MCAO observations of high redshift galaxies will be the infrared follow-up of sub-mm sources, which may hide the bulk of star-formation activity at very high redshifts. Particularly interesting in this regard will be the combination of deep MCAO infrared imaging with sub-mm continuum maps from the ALMA array. Although the full ALMA capability will probably not come on-line until ~2009, the first observations with a limited number of dishes are expected to begin in ~2005. The unique imaging capabilities of ALMA (15 arcsec^2 field with 0".1 resolution) will be well matched to those of MCAO, and allow a pointed survey of dusty starbursts surrounding high redshift (z>3) radio galaxies and QSOs.

3.5 Ages, metal content and structure of distant dwarf galaxies

The origin and evolution of the dwarf galaxies in rich clusters can give us information about the evolutionary processes of the clusters as a whole. There are theories that claim that dwarf galaxies are "failed" galaxies - they never got big enough. Other theories suggest that dwarf galaxies are formed by pieces of larger galaxies that got separated during mergers and interactions. These two possible methods of formation of dwarf galaxies result in very different properties of the stellar populations in terms of ages and metal content. If dwarf galaxies are formed from pieces of larger galaxies, they may have a larger metal content and may also have a different mean age than if they are "failed" galaxies formed on their own from smaller density enhancements.

Very little is known about how the population of dwarf galaxies evolve over time since is it difficult to observe these faint galaxies at redshifts large enough (z up to about one) to address this problem. Further, even when imaging in the optical is done we cannot

distinguish metal variations from age variations for the old stellar population in these galaxies. By "old stellar populations" is meant ages larger than about 2-3 Gyr, e.g. no emission lines. Imaging in the near-IR with AO will give sufficient resolution to study the scale lengths and surface brightness of dwarf galaxies in intermediate redshift clusters ($z \sim 0.2$-1.0). This will give the possibility of addressing the evolution of the structure of this population of galaxies. Further, by combining the near-IR observations with observations in the optical (e.g. HST/WFPC2) we can break the degeneracy of age and metal content. This may make it possible to study how the stellar populations in these galaxies evolve over time and test the models for their evolution in detail.

In order to cover large enough samples of galaxies in an efficient way a field of view that covers the cores of intermediate redshift clusters is needed. A field of view of >1'x1' will do just that. Further, it is a requirement that there are no large PSF variations over the field, since otherwise surface photometry of the galaxies will become very difficult to obtain.

4 COMPARISON OF MCAO WITH CLASSICAL AO

We here describe the results of simulated observations of intermediate redshift galaxies. The purpose of the simulations is to quantify the gains achieved by using MCAO rather than classical AO on Gemini S for the purpose of morphological studies of intermediate redshift galaxies. The central questions are: (1) Can the input profile type be recovered, e.g. $r^{1/4}$ or exponential luminosity profile? (2) Can the input total magnitude be recovered? (3) Can the input half-light radius be recovered?

4.1 A simulated galaxy field at z=0.6

We constructed a simulated galaxy field in which the galaxy sizes and luminosities match observed properties of galaxies at a redshift of 0.6. The projected density of galaxies is higher than found in rich clusters, since the main purpose is to simulate enough galaxies to quantify the gains of MCAO, rather than produce realistic looking simulated cluster images. The galaxy field covers 65"x65". The galaxies have either $r^{1/4}$ or exponential luminosity profiles, but not combinations of the two types.

We concentrate on two subfields, each 16.25"x16.25". The central subfield covers from -4" to 12.25" relative to the optical axis, while the outer subfield covers from 13.65" to 29.9". Thus, the outer-most corner is 42.3" from the optical axis. Each subfield contains three stars. Simulations were made for the classical AO (one 17 mag NGS and one LGS, both located in the center of the field) and for the baseline MCAO system(five LGSs and three 17 mag NGCs). Sky background and noise were added equivalent to an exposure time of 6 hours in the H-band.

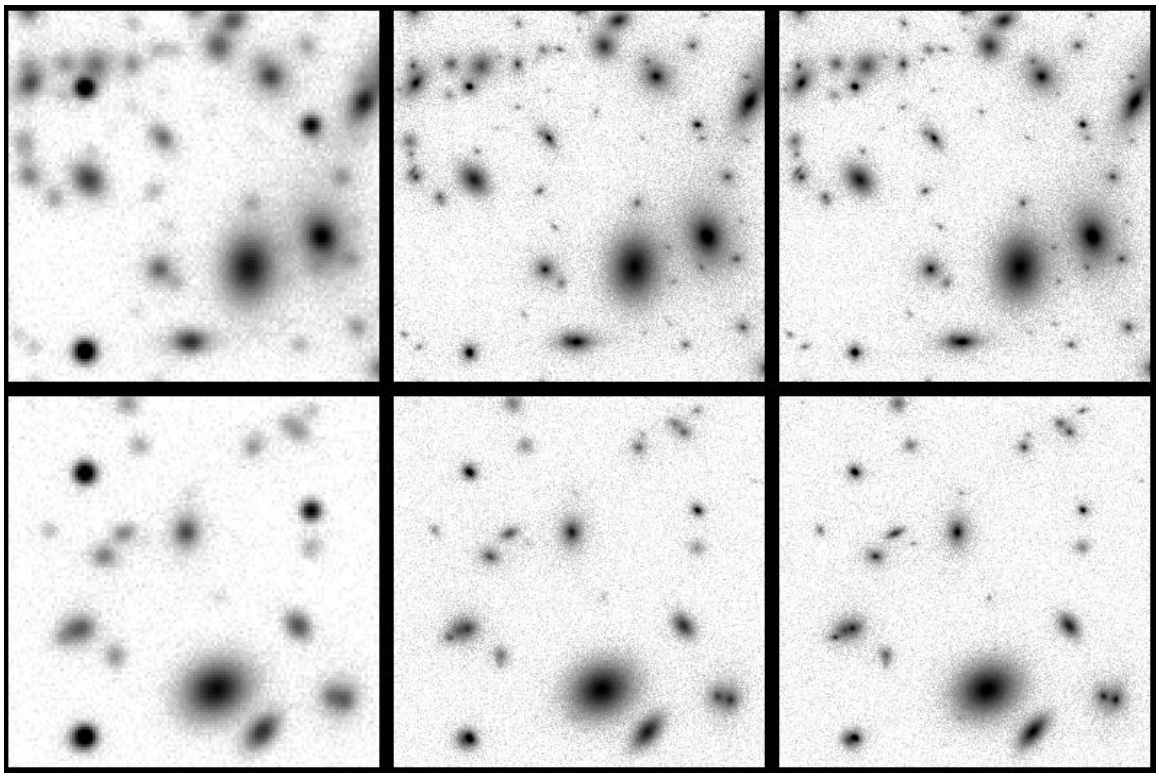

Figure 4.1: Simulated galaxy field at z=0.6. Top row – central subfield. Bottom row – outer subfield. Left – Seeing limited case, fwhm=0.5 arcsec; center – classical AO; right – MCAO. The subfields cover 16.25"x16.25". The pixel size for the seeing limited case is 8 times as large as for the AO and MCAO simulations. This larger pixel size matches the typical pixel scale for non-AO imagers.

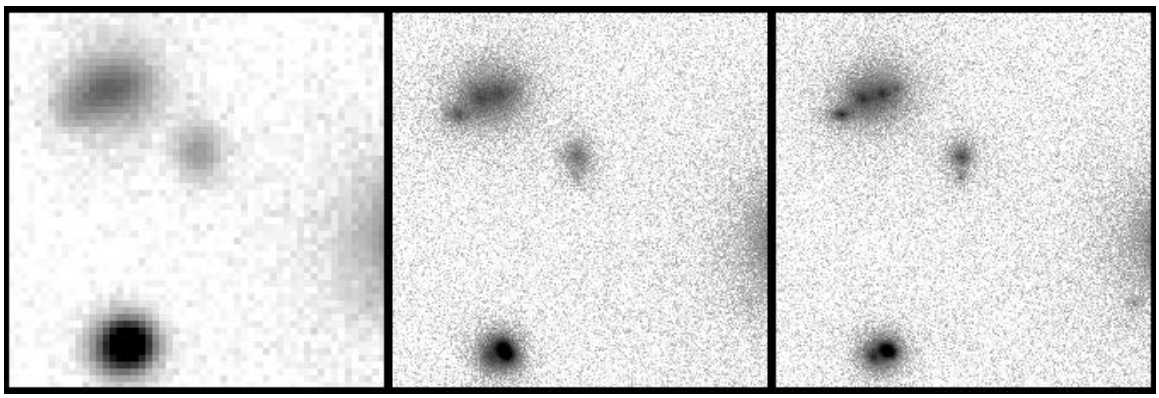

Figure 4.2: A 7"x7" subfield of the simulation, approximately 30" from the optical axis. Left – Seeing limited case; center – classical AO; right – MCAO. The subfield contains eight faint galaxies, one close to the bright star in the lower left. All eight galaxies can easily be identified in the MCAO simulation, while in the simulation of classical AO only five of the galaxies can be identified due to the degradation of the PSF far from the optical axis.

Figure 4.1 shows the simulated fields for the seeing limited case, for classical AO and for MCAO. In Figure 4.2 a smaller area of the outer field located approximately 30" from the optical axis, illustrating the gains in resolution for MCAO compared to classical AO.

4.2 Two-dimensional galaxy fitting

The simulated images were analyzed in a similar way as one would analyze real high spatial resolution imaging data of intermediate redshift galaxies, e.g. imaging data obtained with Hubble Space Telescope. The galaxies brighter than 22 mag in the H-band were fitted with 2-dimensional models convolved with a 2-dimensional point-spread-function (PSF). Each simulated galaxy was fitted twice, with an $r^{1/4}$ and with an exponential profile. The output from the this process consists of the half-light radii, the total magnitudes, the ellipiticities and the position angles for the best fitting models. Further, the goodness of the fit is derived as $\chi^2/N_{pix,}$ where N_{pix} is the number of pixels within the fitting radius and $\chi^2= \Sigma\ (n_i\text{-}n_{i,model})^2/\sigma_i^2$ with the sum over all the pixels within the fitting radius. The three stars in the fields were fitted by scaling of the constructed PSF. All objects in a field are fitted simultaneously. Pixels containing signal from the objects that are not fitted are omitted from the fit. A residual image with the fitted models subtracted aids in the evaluation of the derived fits.

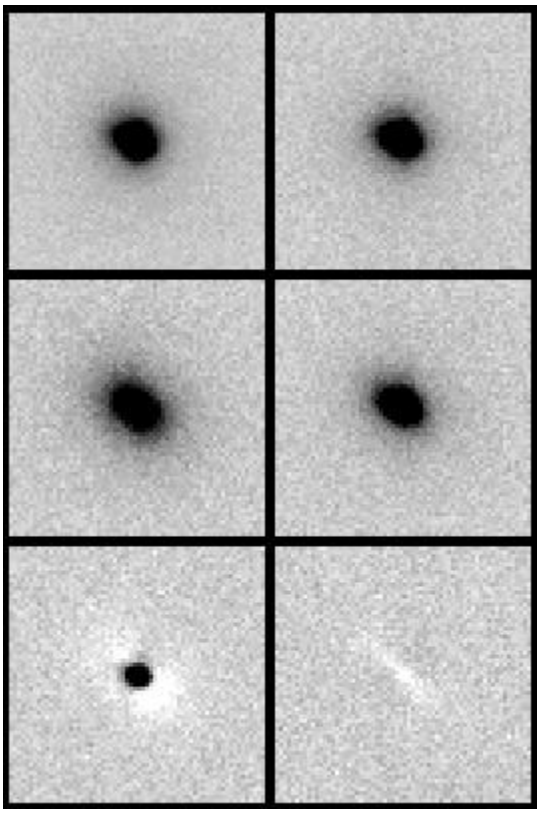

Figure 4.3: The point-spread-functions for the simulations. Left column – classical AO; right column – MCAO. Top row – PSF for the central subfield; center row – PSF for the outer subfield; bottom row – difference between the PSF for the central subfield and the outer subfield. For the classical AO the peak signal in the (normalized) PSF for the outer field is only 40 per cent of the peak signal in the PSF for the central field. The differences between the two PSFs for the MCAO is only about 3 per cent.

The PSFs were constructed from two or all three stars in each of the simulated fields. Figure 4.3 shows the PSFs as well as the difference between the PSFs for the central and the outer field. The large PSF variation with distance from the center of the field is obvious for the classical AO case. For real observations, stars may not be conveniently located in the field. Thus, to illustrate a worst case scenario we also mismatched the PSFs, fitting the outer field using the PSF for the central field and visa versa.

4.3 MCAO versus classical AO

In order to assess whether it is possible to recover the input profile type, we use the goodness of the fit, χ^2/N_{pix}. Figure 4.4 shows χ^2/N_{pix} as a function of the input total magnitude. In Fig. 4.4a and c we have used the correct PSF derived from the same field as the field fitted. For galaxies brighter than about 20.5 mag, fitting the incorrect profile, e.g. an exponential to an input $r^{1/4}$ profile, results in a significantly worse fit than when the correct profile is fitted. Thus, the input profile type can be recovered. In the case of a mismatched PSF (Fig 4.4b and d), the input profile type can be recovered to the same magnitude for the MCAO simulations, while for the simulations of the classical AO the fits become indistinguishable at about 20 mag. This is an expected consequence of the PSF variation over the field for classical AO.

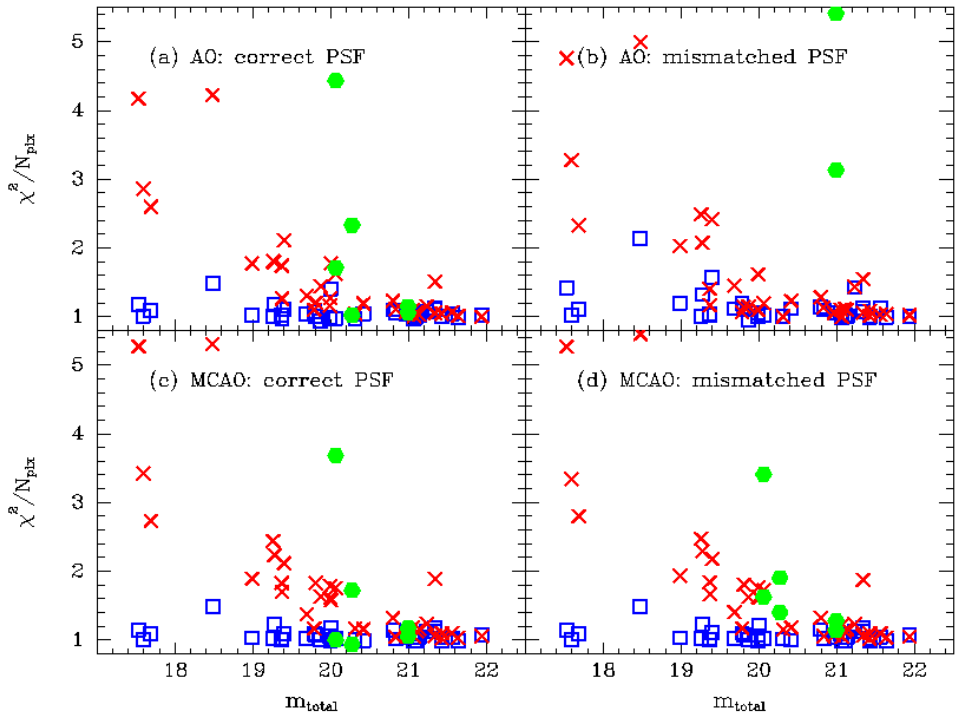

Figure 4.4: The goodness of the fits, c^2/N_{pix}, as a function of input total magnitude. (a) and (c): The correct PSFs were used. (b) and (d): The fits were performed with the mismatched PSFs. Boxes (blue) – the galaxies were fitted with the correct profile type; crosses (red) – the galaxies were fitted with the incorrect profile type. Grey (green) hexagons – results for the stars. In panel (a) and (c) the one star with large c^2/N_{pix} is located very close to a faint galaxy. This star was not included in the determination of the PSF. In panel (b) four of the six stars have c^2/N_{pix} larger than 5.5.

In addition to the goodness of the fits, we may inspect the residual images in order to judge if the correct profile can be recovered. In Figures 4.5 and 4.6 we show the residual images for the fits with $r^{1/4}$ and exponential profiles. For the brighter galaxies the residuals in general show very clearly which of the two profile types is correct, and we

can reliably recover the input profile type. Figure 4.5 also shows the significant PSF variation over the subfields that we are analyzing. The residuals from the stars (marked with black circles) reflect the systematic PSF variation.

Before discussing the results for the total magnitudes and the half-light radii, it is worth keeping in mind that even for nearby bright galaxies, e.g. galaxies in the Coma cluster, the typical random uncertainties on the total magnitudes are of the order 0.1 mag, while the uncertainties on the half-light radii are about 10 per cent. These uncertainties are due to the large (infinite) angular extent of galaxies which means that the total magnitudes and half-light radii must be measured by fitting models to the brighter parts of the galaxies, or alternatively attempt to estimate the parameters from the asymptotic behavior of the enclosed luminosity as a function of aperture size.

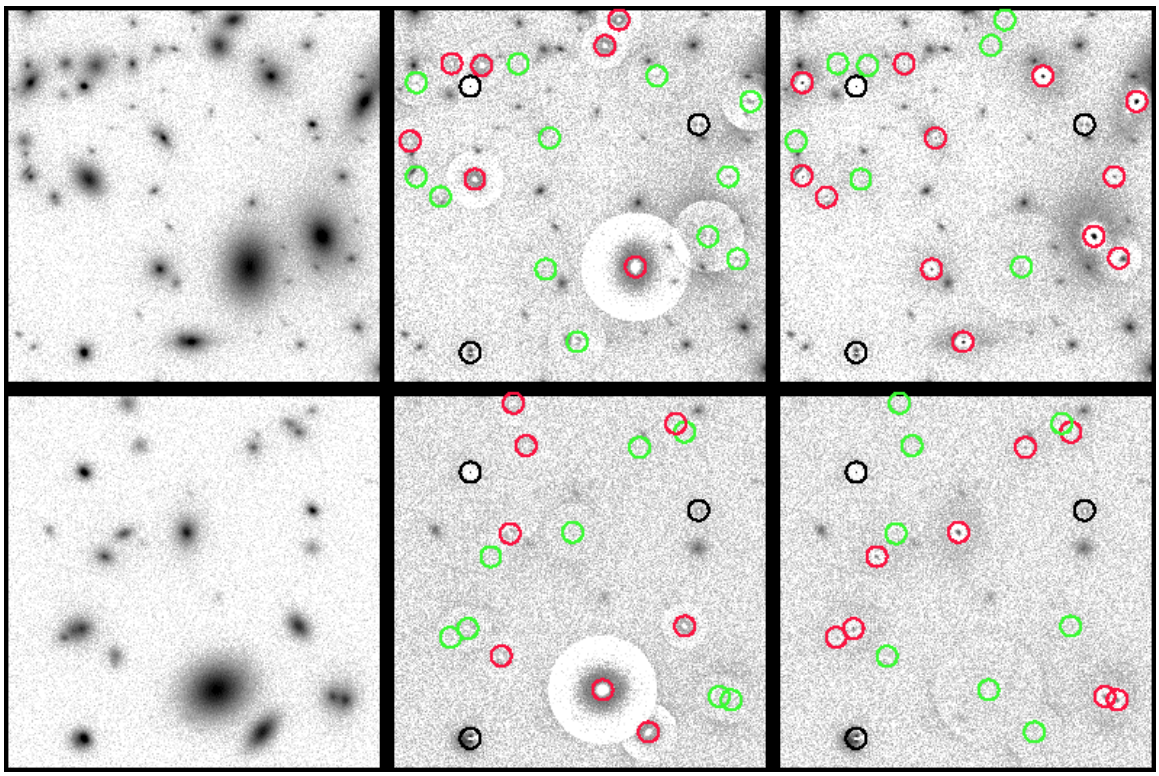

Figure 4.5: Residual images for the simulation of classical AO. Top – central field; bottom – outer field. Left – input simulated image; center – residuals after fitting with $r^{1/4}$ profiles; right – residuals after fitting with exponential profiles. In the residual images galaxies fitted with the same profile type as the input profile are marked with light grey (green) circles, while galaxies fitted with the incorrect profile type are marked with dark grey (red) circles. The three stars in each field are marked with black rings.

Figure 4.7 and 4.8 show the results from the fitting versus the input parameters for the total magnitudes and the half-light radii, respectively. We show the results from fitting the correct profiles, as well as fitting the incorrect profiles. For real data the best fitting profile type would have to be decided on based on the values of χ^2/N_{pix}.

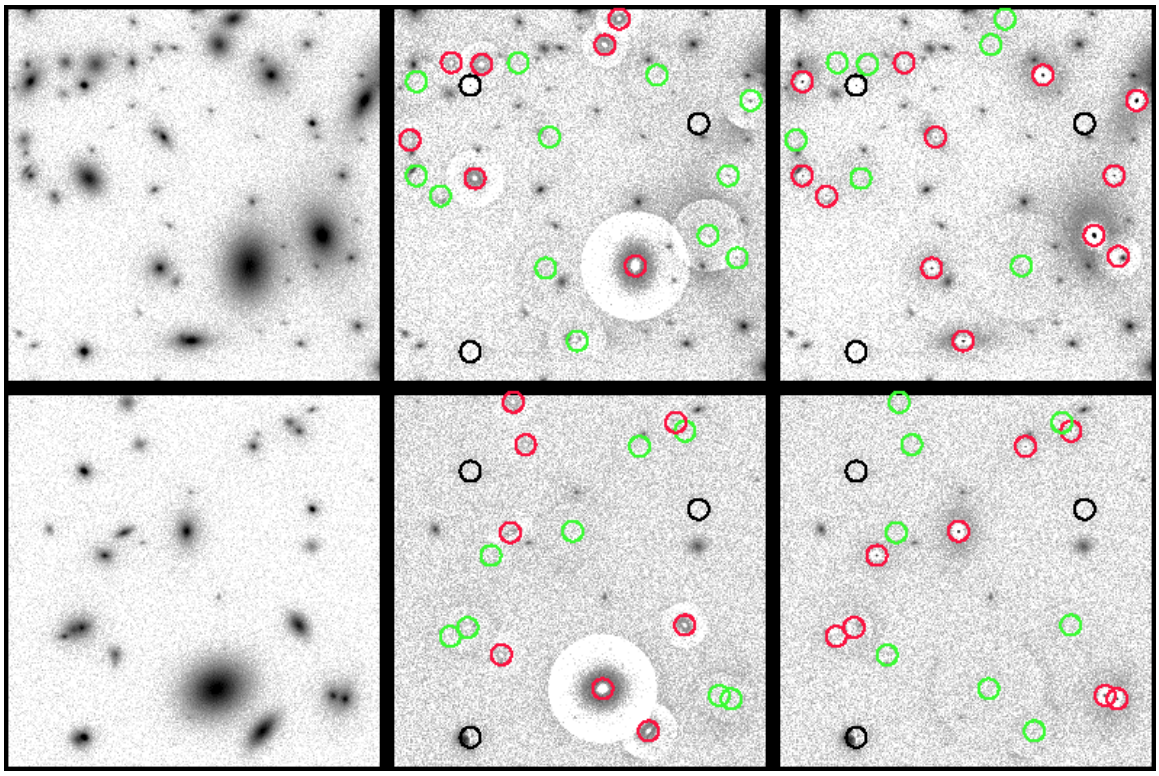

Figure 4.6: Residual images for the simulation of MCAO. Top – central field; bottom – outer field. Left – input simulated image; center – residuals after fitting with $r^{1/4}$ profiles; right – residuals after fitting with exponential profiles. In the residual images galaxies fitted with the same profile type as the input profile are marked with light grey (green) circles, while galaxies fitted with the incorrect profile type are marked with dark grey (red) circles. The three stars in each field are marked with black rings.

The small offsets between the one-to-one relations on Figures 4.6a,c and 4.7a,c and the location of most of the points are due to the limited size of the PSFs used for the fitting. The PSFs include about 88 per cent of the total signal in the stars. The fitting cannot be done with larger PSFs, due to the low signal-to-noise of the stars. For real observations this is a common problem if the available stars in a field are faint as those included in the present simulations. The small size of the PSFs causes the magnitudes for the galaxies to be determined 0.12 mag too faint, and correspondingly the half-light radii is determined too small. For $r^{1/4}$ and exponential profiles an offset in 0.12 mag in the total magnitude corresponds to an offset in the logarithm of the half-light radius of about 0.075. The dotted lines on Figures 4.6a,c and 4.7a,c show the expected relations when the systematics due to the small PSF size have been taken into account. The derived total magnitudes and half-light radii follow these expected relations, with some scatter as expected.

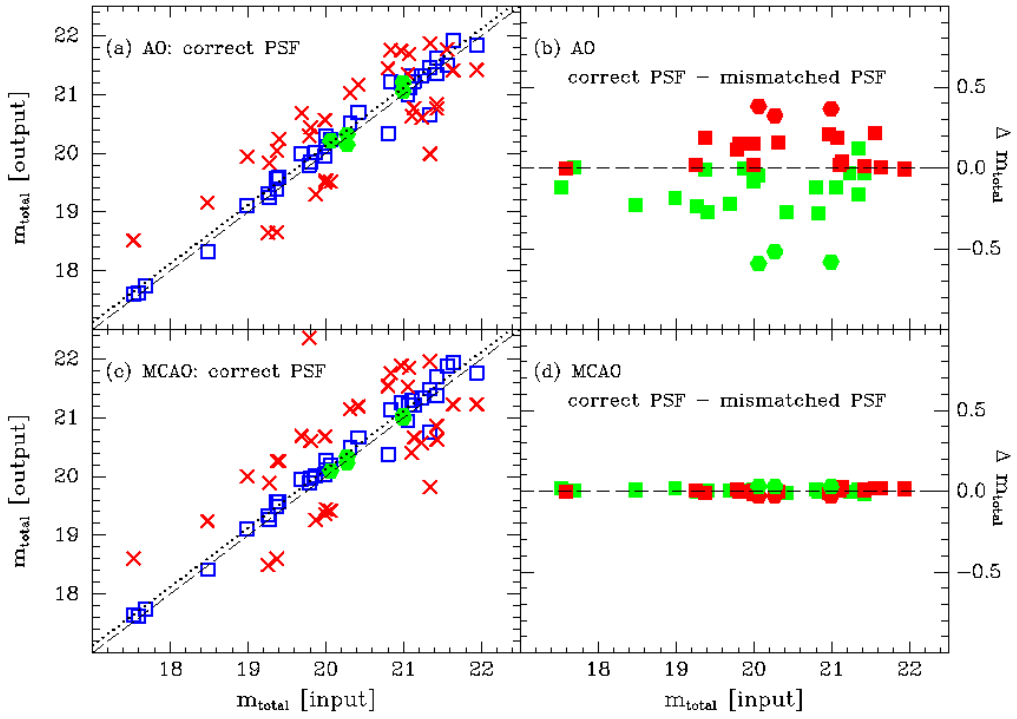

Figure 4.7: The total magnitudes of the galaxies and stars. (a) and (c): The correct PSFs were used. Boxes (blue) – the galaxies were fitted with the correct profile type; crosses (red) – the galaxies were fitted with the incorrect profile type. Grey (green) hexagons – results for the stars. The dashed lines are the one-to-one relations, the dotted lines are the expected relations due to the limited size of the PSF used in the fitting, see text. (b) and (d): The difference between the result when the correct PSF is used and when the mismatched PSF is used. Dark grey (red) – the outer field; light grey (green) – the central field. Boxes – galaxies; hexagons – stars, at +0.4mag and –0.5mag in panel (c). The mismatched PSFs result for the classical AO in systematic errors in the total magnitudes of 0.2-0.3mag for the galaxies (and 0.4-0.5mag for the stars).

For the classical AO, the PSF variation over the field will in general not be fully mapped. It can easily be the case that the PSF is known only from the central NGS. Figures 4.7b,d and 4.8b,d show the effect of using the mismatched PSFs. For the classical AO, this results in systematic errors in the total magnitudes of 0.2-0.3 mag for the galaxies (and 0.4-0.5 mag for the stars), and systematic errors in the half-light radii of 25-50 per cent. For the MCAO simulation no systematic effects result from mismatching the PSFs.

Classical AO can only successfully be used for reliable measurements of half-light radii and total magnitudes of distant galaxies if the PSF is known as a function of position in the field. For a field of view of 1'x1' at high Galactic latitude (where we are most likely to pursue studies of high redshift galaxies) will contain less than five stars bright enough to use for reconstruction of the PSF variation over the field. Thus, in most cases we will have insufficient knowledge of the PSF variation over the field of view. The very small variation of the PSF over the field that is the result of the MCAO is essential for the ability to measure half-light radii and total magnitudes of distant galaxies. The presented simulations show that without MCAO we cannot study galaxy morphology with

quantitative methods over the size field of view (1'x1' or larger) that is necessary for pursuing the science cases outlined in Section 3.

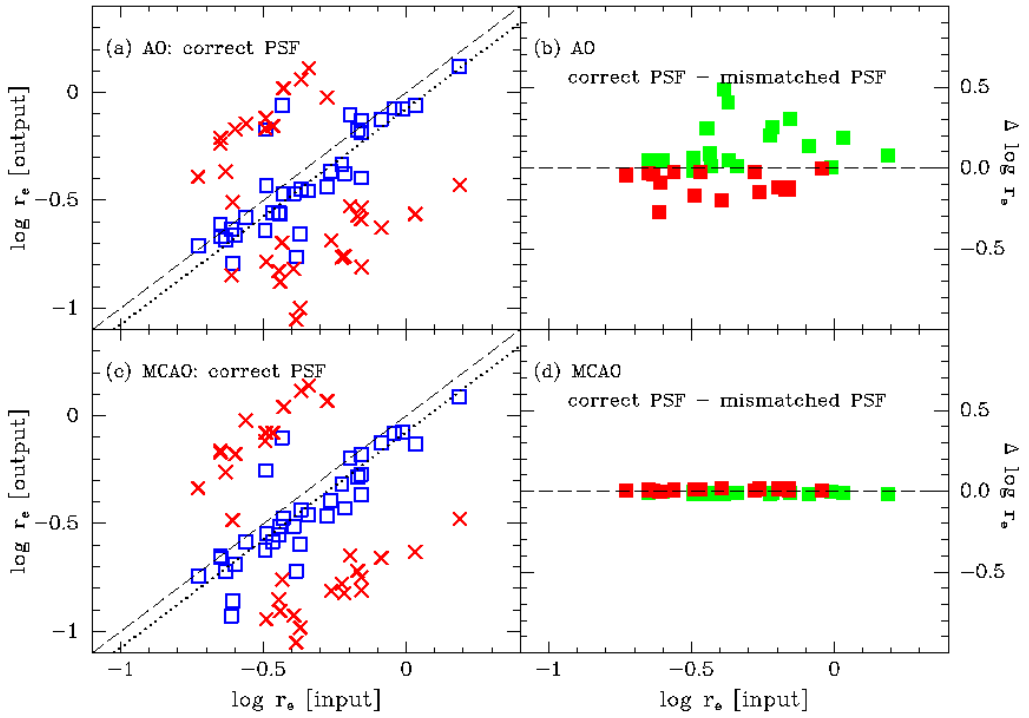

Figure 4.8: The half-light radii of the galaxies. (a) and (c): The correct PSFs were used. Boxes (blue) – the galaxies were fitted with the correct profile type; crosses (red) – the galaxies were fitted with the incorrect profile type. The dashed lines are the one-to-one relations, the dotted lines are the expected relations due to the limited size of the PSF used in the fitting, see text. (b) and (d): The difference between the result when the correct PSF is used and when the mismatched PSF is used. Dark grey (red) – the outer field; light grey (green) – the central field. The mismatched PSFs result for the classical AO in systematic errors in the half-light radii of 25-50 per cent (0.1-0.2 in log r_e).